ACS APPLIED MATERIALS & INTERFACES

Research Article

www.acsami.org

Hydrogen-Bond-Mediated *in Situ* Fabrication of AgNPs/Agar/PAN Electrospun Nanofibers as Reproducible SERS Substrates

Tong Yang,[†] Hui Yang,[†] Shu Jun Zhen,[†] and Cheng Zhi Huang*[,†,‡]

[†]Key Laboratory of Luminescent and Real-Time Analytical Chemistry (Southwest University) Ministry of Education, School of Chemistry and Chemical Engineering, Southwest University, Chongqing 400715, P. R. China

[‡]College of Pharmaceutical Science, Southwest University, Chongqing 400716, P. R. China

Supporting Information

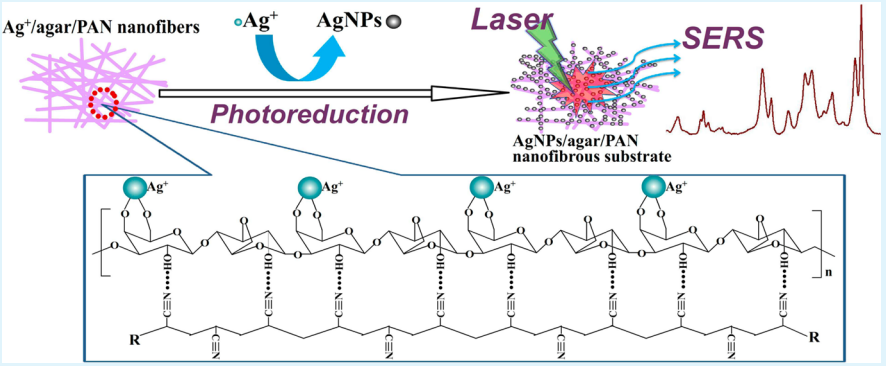

ABSTRACT: Reproducibility in surface enhanced Raman scattering (SERS) measurements is a challenge. This work developed a facile way to make highly dispersed uniform silver nanoparticles (AgNPs) loaded in the agar/polyacrylonitrile (PAN) nanofibers by the coupling the electrospinning technology from metal complex-containing polymer solution and *in situ* photoreductive technique. Agar, as hydrophilic component, was introduced into the electrospinning solution considering that its abundant hydroxyl group sites could greatly improve the contents of silver ions in the polymers because of the rich silver ion chelated with the hydroxyl group, whereas hydrophilic agar was integrated with hydrophobic PAN by −OH···N≡C− hydrogen bonds as a bridge. Meanwhile, the *in situ* photoreductive reaction was made under different light irradiations such as desk lamp, 365 nm UV-lamp, and 254 nm UV-lamp. High yield of stable AgNPs with highly uniform and dispersion are available in the agar/PAN nanofibers after the *in situ* photoreductive reaction, supplying the possibility of reproducible SERS signals. To identify that concept of proof, a facile approach for the determination of malachite green (MG) in three environmental practical samples was demonstrated by using the composite nanofibrous material irradiated by 365 nm UV-lamp, giving the minimum detection concentration of MG as low as 0.1 μmol/L with a good linear response ranging from 0.1−100 μmol/L (R^2 = 0.9960).

KEYWORDS: *agar, hydrogen bonds, in situ photoreduction, reproducible SERS substrates, electrospinning*

INTRODUCTION

SERS is an ultrasensitive, noninvasive, and powerful analytical technique for detecting and identifying specific targets through enhancing Raman signals of molecules located in the vicinity of noble metals or their nanostructures,[1−3] wherein the fabrication of SERS active substrates are crucial. Recently, single-metallic nanomaterial (SMNM) (Au, Ag, Pt, etc.) and semiconductor nanomaterials (CdTe, ZnS, CuO, etc.) as a tremendous potential SERS active substrates have been intensive research upsurge because of their interesting chemical and physical properties such as optical, electrical, magnetic properties.[4−8] Among those metal or metallic compounds nanomaterials, AgNPs exhibit excellent performance in optical absorption, scattering signatures,[9] and the SERS signals by electromagnetic enhancement, which attributes to the local surface plasmon resonances (LSPR).[10]

Hence, considerable attention has been paid to design and fabricate the high SERS active Ag nanocomposite substrates such as rare-earth fluorides/Ag hybrid architectures,[11] "flower-like" AgNPs,[12] core/shell structure,[13] and so forth. To further facilitate and broaden the SERS applications of Ag nanocomposite materials, it is obvious that developing facile and cost-effective methods is essential to fabricate nanostructured SERS substrates with controlling morphologies and structures. Nowadays, a novel way appeared to well-dispersed AgNPs in polymer nanofibers by electrospinning, which has been demonstrated for preparing SERS active substrates.[14]

Electrospinning, as a remarkably flexible and easy technique to fabricate nonwoven nanofibers through an electrically

Received: October 11, 2014
Accepted: December 29, 2014
Published: December 29, 2014

DOI: 10.1021/am507010q
ACS Appl. Mater. Interfaces 2015, 7, 1586−1594

Scheme 1. Schematic Image of Illustrating the Fabrication Process of AgNPs/Agar/PAN Nanofibers and Its Application in the SERS Detection of Malachite Green

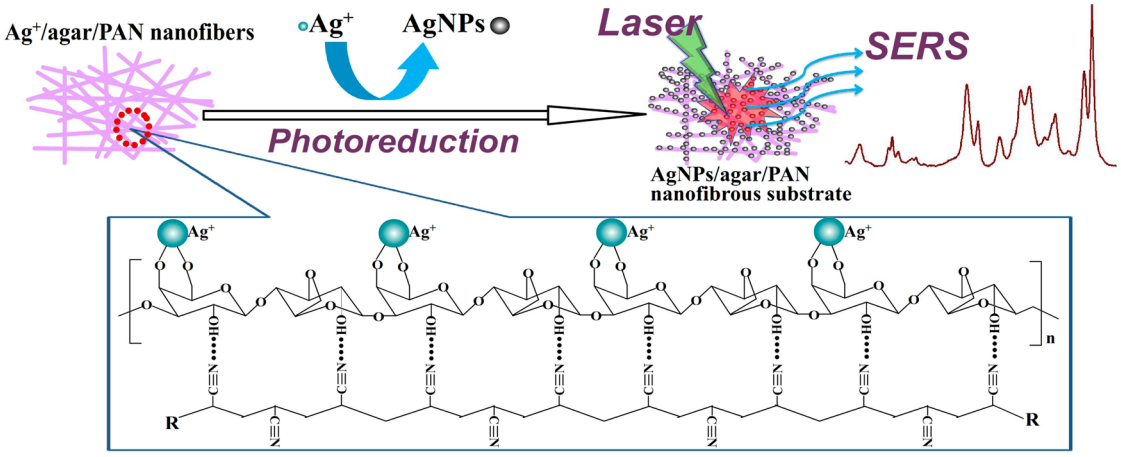

charged jet of a polymer solution, has been widely explored for several decades.[15] This technique have been applied to prepare a rich variety of functional nanofibrous materials and further been applied in biomimetic processes,[16] optoelectronic devices,[17] fingerprint recognition,[18] sensors,[19] immunoassay,[20] environmental fields[21] and so on. Simultaneously, the electrospinning technique also has satisfactory performance on SERS substrates.[14] As compared to the common SERS substrates, the electrospun nanofibers substrates have become significant for fabricating the nanofibers with large surface area to volume ratio, high porosity and excellent mechanical property, which also might improve the SERS performance of hybrid composites.[22] Currently, the assembly methods of functional nanoparticles on the surface of nanofibers have been studied for fabricating the SERS active substrates, such as chemical reduction,[22] electroless plating,[23] e-beam evaporator,[24] metal sputtering coating,[25] and oxygen plasma etching,[26] have been adopted. These methods, however, have some intrinsic disadvantages including tedious steps, changes of the properties of nanofibers and the activity of nanoparticles at high temperature. Otherwise, most of substrates only have been demonstrated theirs SERS ability by several Raman probes molecules, not been actualized theirs applications in practical samples. Therefore, the development of a new strategy for establishing diversified, functional and multicomponent electrospun nanofibrous membranes with high active metallic nanoparticles loading may generate interest in this area.

In our previous study, we have proposed for the first time that agar could be doped into PAN to fabricate antimicrobic material since agar is an ordinary polysaccharide with abundant hydroxyl which has strong affinity toward hydrophilic substances including soluble metallic ions and drugs. The introduction of agar might provide a new route to combine the performance of a hydrophilic phase and a hydrophobic phase, and to improve the drug loading in electrospun nanofibers and promote the sustained release of drug.[27] The most important we suppose is that the strong intermolecular −OH···N≡C− hydrogen bonding interaction in agar/PAN polymers between the hydroxyl sites of agar and the cyano groups of PAN might lay a good foundation for preparing new smart metallic salts/agar/polymer nanofibrous membrane. In such a case, herein we describe an effective route to fabricate AgNPs/agar/PAN nanofibrous membranes with reproducible SERS substrates (Scheme 1) by coupling electrospinning and *in situ* photoreductive technology, and identify the role of the hydrogen bonds. As expected, agar was integrated with PAN by −OH···N≡C− H-bonds as a bridge. The contents and regular distributions of silver ions (Ag^+) in the polymers get improved owing to the chelation between the remanent hydroxyl sites of agar and Ag^+ and thus the *in situ* photoreductive reaction can effectively occur, resulting in high yield of stable AgNPs with highly uniform and dispersion in the agar/PAN nanofibers. The as-synthesized AgNPs/agar/PAN hybrid nanofibrous mats can be used as effective SERS substrates for cost-effective and reproducible SERS applications. What's more, the hydrophobic PAN matrix could keep a certain morphology of the nanofibers under photoreducing process in the atmosphere and after immersing into samples solution comparing with our another work.[28] Importantly, to further stand out the SERS ability, this electrospun composite material has been successfully applied to sensitively and widely detect a cationic triphenylmenthane dye—MG in environmental water samples.

EXPERIMENTAL SECTION

Materials. Polyacrylonitrile powder (PAN, average M_w = 150 000) and malachite green (MG) were purchased from Sigma-Aldrich. *N,N*-dimethylformamide anhydrous (DMF, 99.5%) was obtained from Tianjing Guangfu Technology Development Co. Ltd., which was chosen as a solvent. Agar and *p*-aminothiophenol (*p*-ATP) were acquired from Beijing Dingguo Biological Technology Co. Ltd. and Aladdin Ltd., respectively. Silver nitrate ($AgNO_3$ AR, 99.8%) was purchased from Shanghai Shenbo Chemical Engineering Co. Ltd.. All chemicals were used as-received without further treatment.

Preparation of Electrospun Nanofibers. First, as in our previous work,[27] PAN powders and agar powders were dissolved in DMF to make solutions with concentrations of 7 wt % (w/v, PAN/DMF) and 8 wt % (w/v, agar/DMF), respectively. The mass ratio of agar and PAN is 1.5:1. The former was followed by vigorous stirring to gain a homogeneous and clear polymer solution at room temperature, and the latter was kept at 55 °C under vigorous stirring for completely dissolving. Then the as-prepared agar solution was added into the PAN solution with magnetic stirring for 2 h to achieve a homogeneous and light yellow solution. Then, $AgNO_3$ was added into the above solution with magnetic stirring for 10 h in dark area to avoid the decomposition of $AgNO_3$, which contained 1.5 wt % in the electrospun solution (w/v, 0.1 g $AgNO_3$/solvent). The viscous solution was filled into a 10 mL plastic syringe with a blunt-ended needle whose inner diameter was 0.8 mm. The electrospun nanofibers were prepared using commercial electrospinning equipment. All nanofibers were electrospun under the high-voltage of 20.0 kV, and

DOI: 10.1021/am507010q
ACS Appl. Mater. Interfaces 2015, 7, 1586−1594

the needle was located at a distance of 20 cm from the grounded collector, which was an aluminum plate wrapped with an aluminum foil. The syringe pump was applied to feed solutions to the needle at a rate of 1.8 mm/h. All mats were allowed to dry in air at 40 °C and removed the remanent solvent for terminating electrospinning.

Photoreduction of Silver Ions on Electrospun Nanofibrous Mats. The desk lamp (11 W), the ultraviolet lamps (11 W) with wavelength of 254 and 365 nm were employed as the irradiation sources. The as-prepared electrospun mats were divided into three equal segments, and illuminated for a certain time under the lamps above, respectively. This progress was strictly performed in darkroom to keep away from other kinds of luminous beams. Finally, the electrospun AgNPs/agar/PAN nanofibers were prepared on the basis of the explicit protocol above. Meanwhile, the $AgNO_3$/agar/PAN nanofibrous mats before illuminating could be regarded as control alone.

Characterization. The morphologies and diameters of the as-prepared nanofibers and AgNPs were imaged by using a scanning electron microscopy (SEM, S-4800, Hitachi, Japan). The elemental composition of samples was analyzed using an X-ray energy-dispersive spectroscopic (EDS) detector attached to the SEM. Transmission electron microscopy (TEM, JEM-2100, JEOL, Tokyo, Japan), with the selected area electron diffraction (SAED) achieving the situ morphology and crystallographic properties of crystal samples. X-ray powder diffraction (XRD) patterns were obtained by a Shimadzu XRD-7000 (Beijing Purkinje General Instrument Co. Ltd.) with Cu–Kα (1.5405 Å) radiation source under the operating voltage and current of 40 kV and 50 mA. X-ray photoelectron spectroscopy (XPS) analysis was performed on an ESCRLRB250X (America) cispectrometer with a standard Al K source ($h\nu$ = 1486.6 eV). Functional groups analysis of fibrous mats was recorded by a Fourier transform infrared Spectrometer (Shimadzu, 8400S, Japan) from 4000 to 600 cm^{-1} at room temperature. Nuclear magnetic resonance (NMR) spectra were recorded on AVANCE AV-400 (BRUKER, Swiss) with the reference of ^1H NMR chemical shifts of the residual solvent peak at 2.50 ppm in DMSO-*d6*.

SERS Performance. In this SERS study, *p*-ATP was used as the probe molecule. Five μL of *p*-ATP aqueous solutions with concentration of 1.0×10^{-4} M was prepared by drop-casting 9 mm^2 of AgNPs/agar/PAN hybrids nanofibers attaching to the silicon substrates. Then, SERS spectra of *p*-ATP (1.0×10^{-4} M) and solid *p*-ATP were acquired at randomly selected spots on the substrates. Finally, we could calculate the SERS enhancement factor (EF). Laser wavelength, 532 nm; power, 28 mW; lens, 50× objective; acquisition time, 5 s.

SERS Detection of MG in Environmental Waters with the Developed Substrate. The representative MG detection procedure was carried on as follows. Typically, eight same size pieces of AgNPs/agar/PAN nanofibers meshes were soaked in 1 mL of MG solutions with varying concentrations containing: (a) 100 μmol/L, (b) 50 μmol/L, (c) 20 μmol/L, (d) 10 μmol/L, (e) 5 μmol/L, (f) 2 μmol/L, (g) 1 μmol/L, (h) 0.1 μmol/L for 4 h. Afterward, the fibrous meshes were tiled at the appropriate size of silicon pellet from taking out of the above solutions. The substrates were left to dry at room temperature before SERS measurements. Ultimately, a linear standard curves was obtained in line with the SERS intensity to the concentration of standard samples.

Considering that there were some illegal use of MG in pisciculture and discharge in industrial waste, we took three types of samples of MG to test our developed substrates for SERS detections. The real water samples were acquired from local fishery water in Beibei, Chongqing (sample 1); lake water in Southwest University, Chongqing (sample 2); and river water at Beibei Whart of Jialing River, Chongqing (sample 3). The impurities of the collected water samples were filtered by 0.45 μm filter film after boiling and then stored at room temperature. The SERS measurements for MG were taken by the same procedures as that of standard samples. All experiments were performed in triplicate.

RESULTS AND DISCUSSION

Morphologies of As-Prepared AgNPs/Agar/PAN Nanofibers. To study the morphologies of the as-fabricated hybrid nanofibers and AgNPs immobilized on nanofibers, we carried out typical SEM and TEM measurements. Figure 1

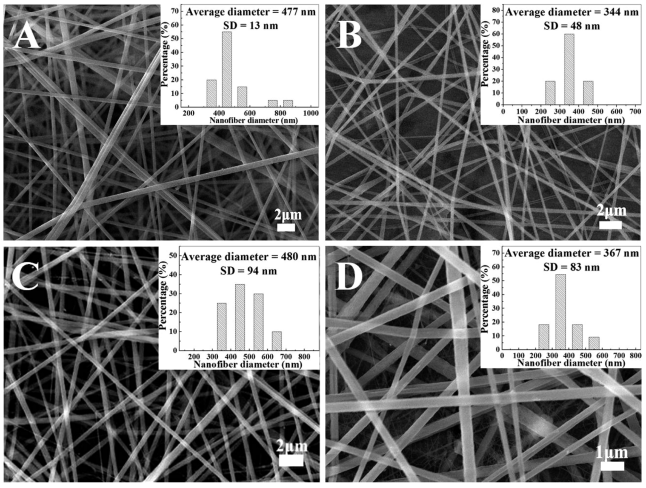

Figure 1. SEM images and morphology of electrospun nanofibers: (A) PAN only, (B) agar/PAN, (C) $AgNO_3$/PAN, (D) $AgNO_3$/agar/PAN before illuminated, respectively. The insets are the corresponding size distribution histogram of the above nanofibers.

shows the SEM pictures of PAN only, agar/PAN, $AgNO_3$/PAN, $AgNO_3$/agar/PAN before illuminated, respectively. It was found that all the nanofibers exhibited a smooth surface, uniform diameters, and highly porous structure, which was beneficial to enhance the surface area-to-volume ratio of the nanofibers membranes. The insets are the corresponding size distribution of the above nanofibers whose average diameters are 477 ± 13 nm, 372 ± 71 nm, 480 ± 94 nm, and 367 ± 83 nm, respectively. After introducing agar in electrospun precursor solution, the diameters of composite nanofibers were thinner than before, which can be attributed to the viscosity and the conductivity of the electrospun solution according to our previous work.[27]

Figure 2A–C depict the SEM images of the as-fabricated AgNPs/agar/PAN nanofibrous membranes, which are illuminated under desk lamp, 365 nm UV lamp, 254 nm UV lamp, respectively. Similarly, these nanofibers performed uniformed diameter, a flat and smooth appearance. Interestingly, a large number of small and spherical AgNPs can be observed on the surface of agar/PAN fibers illuminated by both 365 nm UV-lamp and desk lamp, whereas little AgNPs were observed with the 254 nm UV-lamp. It is assumed that the wavelength and energy of light might play a key role on the reduction of Ag^+. For the sake of exploring more detailed information about the morphology and crystal structure of the AgNPs, TEM and SAED observation were conducted. As shown in Figure 2 D, it is obvious that the well-dispersed small AgNPs embedded in the agar/PAN nanofibers with a uniform average diameter of 7.6 ± 1.7 nm under the condition of 365 nm UV lamp. The SAED results demonstrated that AgNPs contains the face-centered-cubic (*fcc*) crystal structures including single and multicrystal (the top right inset of Figure 2D). The above results indicate that the different irradiations could have an impact on the morphologies and diameters of AgNPs on agar/PAN nanofibers.

DOI: 10.1021/am507010q
ACS Appl. Mater. Interfaces 2015, 7, 1586–1594

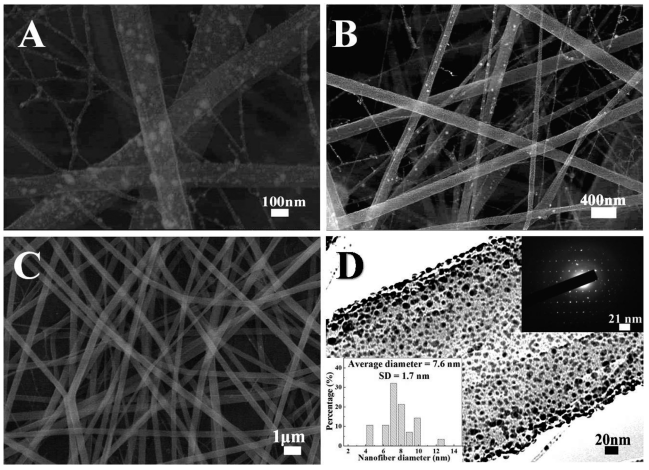

Figure 2. SEM images of the electrospun nanofiber mats from the AgNPs/agar/PAN solution, which had been illuminated by different light sources for 24 h. (A) 365 nm UV lamp, (B) desk lamp, (C) 254 nm UV lamp. TEM images of AgNPs/agar/PAN nanofibers: (D) 365 nm UV lamp, the lower left inset is the corresponding diameter distribution histogram of the immobilized AgNPs, the top right inset is the SAED result of the immobilized AgNPs.

The comparative photograph images of AgNPs/agar/PAN nanofibers membranes before and after photoreduction with the same illuminated time are revealed in the Supporting Information (Figure S1 in the Supporting Information). It presents that the control sample before illuminating is cream white (Figure S1D in the Supporting Information), the samples with desk lamp and 254 nm UV lamp are yellow (Figure S1A, C in the Supporting Information), and the one with 365 nm UV lamp is brown yellow. From the surface plasmon resonance (SPR) absorption of the AgNPs (Figure S1E in the Supporting Information), light irradiations certainly acts as a crucial role in the formation of AgNPs during *in situ* photoreduction.

Characterization of AgNPs/Agar/PAN Composite Nanofibers. To further understand the crystal structure of AgNPs, we measured the XRD patterns of the AgNPs/agar/PAN composite nanofibers (Figure 3 A). A typical XRD pattern of the as-prepared AgNPs shows the diffraction peaks with 2θ values centered at around 38.2°, 44.2°, 64.4°, and 77.4°, which respectively correspond to the (111), (200), (220), and (311) (specific for elemental Ag were present) crystallographic planes of the fcc structure of Ag^0. These results indicate that silver nanoparticles were successfully attached on the agar/PAN polymer matrix.

The chemical composition and electronic structures of the as-prepared AgNPs/agar/PAN mats were analyzed by XPS. As shown in Figure 3 B, it can be clearly observed that the peaks of Ag, C, N and O exist in the sample of AgNPs/agar/PAN mats. The high-resolution XPS spectrum of Ag 3d orbital region shows the binding energies of Ag $3d_{5/2}$ and Ag $3d_{3/2}$ peaks at 367.1 and 372.9 eV from the inset of Figure 3B, respectively. The splitting of the 3d doublet is 5.8 eV, indicating the metallic nature of Ag. Interestingly, the peak of 3d in our work was found to shift obviously to the lower binding energy, indicating that the oxidation of silver might exist in the hybrid composition. Also, the high-resolution XPS spectra for the C 1s region around 285.1 eV was assigned to C−C groups. The peak located at 398.2 eV standing for N 1s that is from cyano groups of PAN. The O 1s chemical states of −OH in agar/PAN mats loacated at 532.6 eV, but the peak of −OH in AgNPs/agar/PAN mats loacated at 532.0 eV, which is mainly attributed to the decreased electron cloud density of O in −OH of agar suggesting that O chelated with silver ions (Figure 3C, D).[29,30]

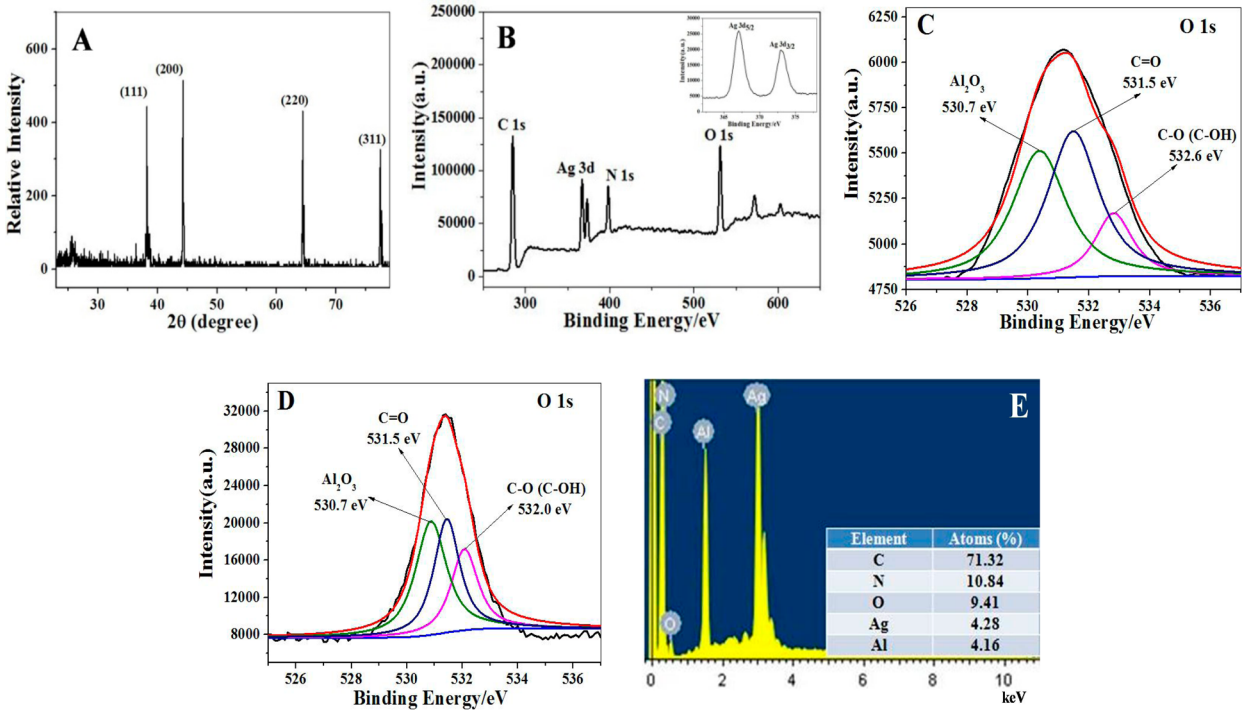

Figure 3. Characterizations of the AgNPs/agar/PAN nanofibers irradiated by UV 365 nm. (A) XRD pattern; XPS spectra of the as-fabricated nanofibers: (B) XPS fully scanned spectra of AgNPs/agar/PAN nanofibers and the inset is the XPS spectra of Ag 3d, XPS spectra of O 1s (C) agar/PAN nanofibers and (D) AgNPs/agar/PAN nanofibers; (E) EDS spectrum of AgNPs immobilized into the AgNPs/agar/PAN nanofibers.

DOI: 10.1021/am507010q
ACS Appl. Mater. Interfaces 2015, 7, 1586−1594

The other two chemical states (531.5 and 530.7 eV) of O 1s were assigned to C═O and Al_2O_3, which originated from the residual solvent and aluminum foil.[31] EDS analysis on the hybrid nanofibers (Figure 3E) evidence the dominance of the element Ag, and further demonstrates that the AgNPs were successfully synthesized and immobilized in the agar/PAN nanofibers. The elemental carbon, nitrogen and oxygen might be from the polymer PAN and agar, even probably from the silver oxide. Aluminum was detected, mainly from the aluminum foil wrapped with the collector.

FTIR analysis displayed that there are big differences of functional groups of PAN, PAN/agar, $AgNO_3$/agar/PAN nanofibrous mats before and after illumination (see Figure S2A in the Supporting Information). Typical absorption at approximately 3460 cm^{-1} for pure agar was attached to the stretching vibration of −OH in agar. The characteristic absorption corresponding to the oxygen functionalities includes the stretching vibration of C−O−C bonds at 1066 cm^{-1} and a coupling of the two C−O stretching modes of the 3,6 anhydrous bridge at 933 cm^{-1}, respectively (Figure S2A(a) in the Supporting Information).[32] In the FTIR spectra of the PAN mats (Figure S2A(b) in the Supporting Information), the salient absorptions has the assignments at the wavenumbers of 2944, 1452, 2247, and 1640 cm^{-1} for the $-CH_2$ asymmetric stretching vibration, bending vibration, −C≡N stretching vibration, and C−O valence vibration, respectively. Wherein, the existence of the above functional groups in the agar/PAN, $AgNO_3$/agar/PAN, and AgNPs/agar/PAN nanofibers was confirmed (Figure S2A(c)—(e) in the Supporting Information). However, the absorption peak of −OH (3460−3433 cm^{-1}) and −C≡N (2247−2236 cm^{-1}) groups shifted to lower wavenumbers. This can be explicated by the strong hydrogen bonding interactions between the −OH of the hydrophilic agar and the −C≡N of PAN medium.[33,34] In addition, it is noteworthy that, as compared with the spectrum of $AgNO_3$/agar/PAN mats (Figure S2A(d) in the Supporting Information), a new, strong and incisive peaks around at 1384 cm^{-1} (Figure S2A(e) in the Supporting Information) appeared after AgNPs loaded on the agar/PAN composition by photoreducing. We speculated that a new functional group might form after loading AgNPs. Similarly, the same position appears as well as strong and incisive peaks under three different irradiations (Figure S2B in the Supporting Information). The $AgNO_3$/agar/PAN nanofibrous membranes after being illuminated by different light sources have strong and sharp peaks at 1384 cm^{-1}, which are consistent with the former discussions. Especially, the hybrid composited mats illuminated by the 365 nm UV lamp are remarkable, comparing with other irradiations.

The hydrogen reaction of hydrophilic agar and hydrophobic PAN is a key step in all process. Thus, ^1H NMR (400 MHz, DMSO-*d*6) spectroscopic measurements of the PAN, agar and agar/PAN solutions can give clear evidence for the formation of the hydrogen reaction between agar and PAN (Figure 4). PAN (Figure 4A): δ (ppm) 3.1624, 3.1371, 3.1186; agar (Figure 4B): δ (ppm) 5.1730, 4.9898, 4.7744, 4.6020, 4.4039, 4.2744, 4.1112, 3.6806, 3.4601; agar/PAN (Figure 4C): δ (ppm) 5.2018, 5.0748, 4.8072, 4.6314, 4.5084, 4.4311, 4.1955, 3.7815, 3.5394, 3.1436, 3.1371, 3.1161. Comparing with PAN solution and agar solution, downfield shifts of the protons of −OH in agar/PAN mixture solution occur. The obvious downfield shifts of the chemical shift in ^1H NMR verify the formation of the H-bonds surroundings in both agar and PAN, which is in accordance with the previous research.[27]

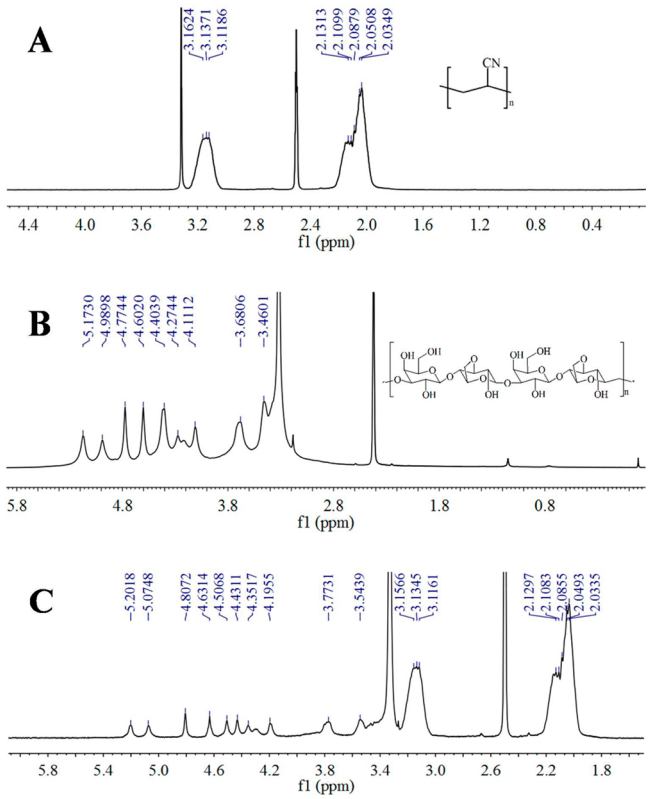

Figure 4. Characterization of the formation of H-bonds: ^1H NMR spectrum of (A) PAN, (B) agar, and (C) agar/PAN. The reference of ^1H NMR (400 MHz) chemical shifts of the residual solvent peak was at 2.50 ppm in DMSO-*d*6.

Role of Agar Introduced in $AgNO_3$/PAN System. First of all, in the experiment process for fabricating AgNPs/PAN nanofibers: when the solid silver nitrate was mixed with PAN solution, it is supposed that the silver ions (Ag^+) and cyano groups of PAN could form chelating complex through the chelating effect between Ag^+ and cyano groups, which contained a pair of long pair electrons in the orbital of N atom.[35] However, there were no obvious nanoparticles on the surface of as-fabricated electrospun material after photoreduction with three different light sources (Figure S3 in the Supporting Information). Besides, AgNPs/PAN nanofibrous substrates show a poor SERS signal for MG comparing with the following AgNPs/agar/PAN nanofibrous substrates (Figure S4 in Supporting Information).

To obtain more AgNPs embedded in the surface of nanofibers, hydrophilic agar solution was added into pristine PAN solution (as shown in Scheme 1). In the typical experiments for fabricating AgNPs/agar/PAN nanofibers, we initially blended agar solution with PAN solution. Because agar is a hydrophilic compound with abundant hydroxyl groups, which can easily react with the cyano groups of PAN to form intermolecular hydrogen bonds of −OH···N≡C−. Thus, functional molecular agar was integrated with PAN by these hydrogen bonds as a bridge.[30,32,33] Ag^+ could coordinate with cyano groups when $AgNO_3$ was added into the mixture, along with the existence of the chelating effect between hydroxyl groups and silver ions,[28,29] so that *in situ* photoreductive reaction could occur. Therefore, Ag^+ ions were gradually reduced to metallic silver when the $AgNO_3$/agar/PAN membranes were irradiated by different light sources, and the

DOI: 10.1021/am507010q
ACS Appl. Mater. Interfaces 2015, 7, 1586−1594

AgNPs gradually formed and dispersed on the surface and internal electrospun nanofibers. TEM image of the formed AgNPs (Figure 2D) showed that AgNPs were well-distributed on the agar/PAN composite fibers and there was no any agglomeration.

The corresponding reaction of generating AgNPs could be depicted as the following reactive processes:[28,36,37] (1) the partial Ag^+ ions were dispersed homogeneous in solution by chelated effect and reduced to tiny Ag atoms as seeds by the aldehyde group of DMF; (2) the rest of Ag^+ might be adsorbed around the surface of nuclei, which were potential foreshadowing for the following photoreduction; (3) photochemical reactions

$$2Ag^+ + 2NO_3^- \xrightarrow{h\nu} 2Ag^0 + 2NO_2 + O_2$$

$$mAg^0 \xrightarrow{h\nu} (Ag)_m$$

the Ag^+ on the surface of nuclei were reduced into Ag atoms by irradiating, which further could promote the formation of nanoparticles. Wherein, the formation of AgNPs on agar/PAN nanofibers under the irradiation of 365 nm UV lamp was remarkable from the SPR absorption (Figure S1E in Supporting Information) and the following SERS activity (Figure S4 in Supporting Information).

As a result, agar in the $AgNO_3$/PAN system served not only as coordination agent but also as stabilizing agent and protective agent to lay the good foundation for the formation of AgNPs at last. Moreover, the simple and green treatment of irradiation played a major role in further forming AgNPs embedded in the nanofibers.

SERS Activity of AgNPs/Agar/PAN Composite Mats as Substrates. Considering that AgNPs can enhance Raman signal through the electromagnetic enhancement mechanism,[38] we chose *p*-ATP as a probe molecule to evaluate the SERS activity of the as-prepared substrates, (Figure S5 in the Supporting Information). *p*-ATP is one of the conventional and ideal analytes in the SERS measurement, it has a distinct Raman property and most of the prominent Raman bands have been assigned.[39] Figure 5 (a, b) show the normal Raman spectra of the solid *p*-ATP and the SERS spectra of the *p*-ATP (1.0×10^{-4} M) adsorbed on the surfaces of AgNPs/agar/PAN nanofibrous mats. The main Raman peaks for solid *p*-ATP (Figure 5 a) are located at 1094 and 1598 cm^{-1}, which are attributed to the ν(C−S) stretching mode and ν(C−C) ring-breathing, respectively.[40,41] In the SERS spectra (Figure 5b), four significant strong bands, δ(C−H) at 1148 cm^{-1}, ν(C−C) + δ(C−H) at 1396 cm^{-1}, δ(C−H) + ν(C−C) at 1443 cm^{-1}, ν(C−C) at 1583 cm^{-1} preferably demonstrate the band positions for the b_2 bending modes.[39,40] These results demonstrate that *p*-ATP can well adsorb the surface of AgNPs/agar/PAN mats. Finally, to investigate the enhancement effect of *p*-ATP on the hybrid nanofibers, band at 1443 and 1583 cm^{-1} were selected as the representation for estimating the SERS enhancement factor (EF) values of *p*-ATP.

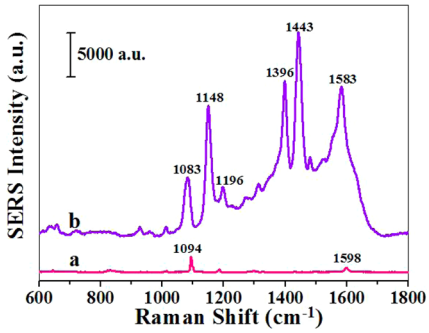

Figure 5. (a) SERS spectrum of *p*-ATP (1.0×10^{-4} M) recorded on randomly selected spots on the surface of AgNPs/agar/PAN nanocomposite mats by the UV 365 nm irradiating and (b) normal Raman spectrum of solid *p*-ATP. Laser wavelength, 532 nm; power, 28 mW; lens, 50× objective; acquisition time, 5 s.

The EF value is estimated using the following equation[42]

$$EF = (I_{SERS}/N_{SERS})/(I_{NR}/N_{NR}) = \frac{I_{SERS}N_{NR}}{I_{NR}N_{SERS}}$$

where I_{SERS} stands for the intensities of the same vibrational mode in the SERS spectrum of *p*-ATP and I_{NR} stands for the normal Raman spectra of solid *p*-ATP. N_{SERS} and N_{NR} are the number of *p*-ATP molecules adsorbed on the SERS substrate and bulk molecules illuminated by the laser focus spot under SERS and normal Raman conditions, respectively. EF of the above b_2 mode, which give rise to the peaks at 1443 and 1583 cm^{-1} were estimated to be 3.1×10^5 and 1.3×10^4, respectively (details can be found in the Supporting Information).

Additionally, we used the as-prepared hybrid nanofibers as SERS substrates to testify again the effect of agar in $AgNO_3$/PAN system through Raman signals by choosing MG as a test molecule. MG standard solution with 1.0×10^{-5} mol/L was placed on the AgNPs/PAN and AgNPs/agar/PAN substrates illuminated by different light sources, and the Raman spectra illustrated the efficiency of the SERS substrates (Figure S4 in the Supporting Information). Finally, we conclusion that (1) the SERS intensity of MG in the presence of AgNPs/agar/PAN nanofibrous mats was much stronger than that of in the presence of AgNPs/PAN nanofibrous mats; (2) the intensity of SERS in the presence of AgNPs/agar/PAN mats prepared under 365 nm UV lamp and desk lamp were much stronger than that of those prepared under 254 nm UV lamp; (3) no Raman signal could be detected on the mats without any photoreduction, which demonstrated that more AgNPs on the agar/PAN mats would be induced after illuminating.

Reproducible SERS Signals of the AgNPs/Agar/PAN Composite Mats as Substrates. As we all known, the good reproducibility of SERS signals about as-prepared substrates is a prerequisite for SERS analysis and is estimated by the relative standard deviation (RSD) of the chief SERS peaks of probe molecules.[43,44] Thus, to test whether the AgNPs/agar/PAN nanofibrous mats could obtain reproducible Raman signals, SERS spectra of *p*-ATP (1.0×10^{-4} M) molecules and MG (1.0×10^{-5} M) molecules from 15 randomly selected locations on the as-fabricated mats were recorded, respectively (Figure 6). Then, the RSD values of main characteristic peaks on *p*-ATP and MG were calculated and presented in Tables 1 and 2, respectively. All RSD values with less than 22% showed the preferable reproducibility across the entire AgNPs/agar/PAN area. At the moment, these results indicate the overall uniformity and reliability of the nanofibrous mats as SERS substrates. From the lowest RSD in Table 2, the characteristic peak at 1618 cm^{-1} could be used for the MG detection. Besides, the morphology of AgNPs/agar/PAN composite nanofibers after immersing into MG solution have no serious changes and no great influence upon the reproducibility of nanofibrous mats (Figure S6 in the Supporting Information).

DOI: 10.1021/am507010q
ACS Appl. Mater. Interfaces 2015, 7, 1586−1594

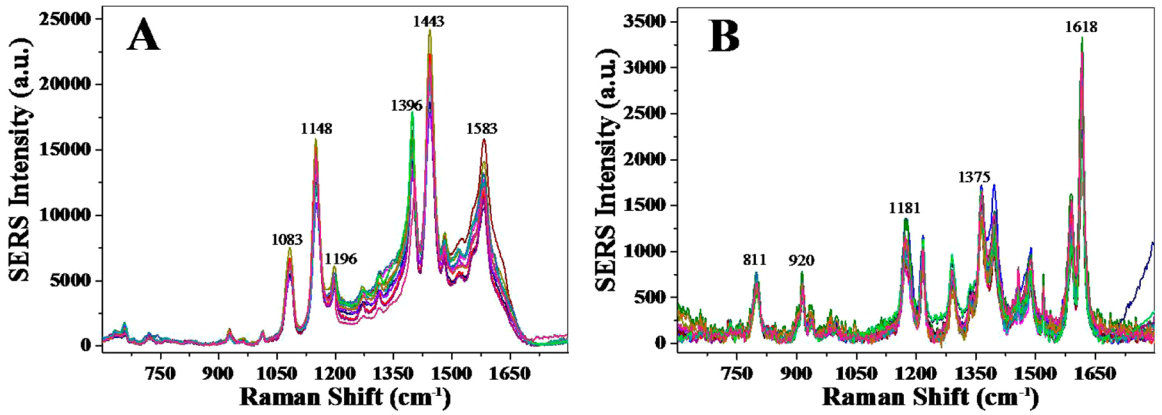

Figure 6. Preferable reproducibility as demonstrated by the overlapping spectra were recorded by AgNPs/agar/PAN nanocomposite mats under the UV 365 nm irradiating. SERS spectrum of (A) *p*-ATP (1.0×10^{-4} M) and (B) MG (1.0×10^{-5} M) recorded on 15 randomly selected spots on the surface of as-prepared AgNPs/agar/PAN nanocomposite mats. Laser wavelength, 532 nm; power, 28 mW; lens, 50× objective; acquisition time, 5 s.

Table 1. RSD Values of the Characteristic Peaks for the *p*-ATP (1.0×10^{-4} M) SERS Spectrum

peak position (cm^{-1})	1083	1148	1196	1396	1443	1583
RSD values (%)	9	11	9	13	8	11

Table 2. RSD Values of the Characteristic Peaks for the MG (1.0×10^{-5} M) SERS Spectrum

peak position (cm^{-1})	811	920	1181	1375	1618
RSD values (%)	16	22	17	15	12

MG Detection in Environmental Water. As a cationic triphenylmenthane dye, MG has been used in the aquaculture, textile, and paper industry and is prohibited in certain countries for its genotoxicity and carcinogenicity.[42,45] As described in Figure 6B, the prominent Raman bands of MG were collected, such as 1618, 1375, 1181, 920, and 811 cm^{-1}, which were ascribed to C−C ring stretching, *N*-phenyl stretching, C−H ring in-plane bending, C−H out-of-plane bending, and C−H out-of-plane bending, respectively.

On the basis of the above results, we chose the AgNPs/agar/PAN mats under 365 nm UV lamp as substrates for MG detection experiment. It could be seen from Figure 7 that the SERS intensity increased with the increase of MG concentration. The SERS peak at 1618 cm^{-1} was used for the quantification, which revealed a good linear SERS response ranging from 0.1 μmol/L to 100 μmol/L of MG ($R^2 = 0.9960$) (the inset in Figure 7). Considering that the as-fabricated nanocomposites have a high enhancement effect, they could be served as a potential SERS sensor for detecting environmentally pernicious substances. To further assess the accuracy of the proposed measurement, it was performed to the determination of MG in a fishery, lake and river water samples, and the researches of recovery were conducted. The recoveries were between 92.0− 105.4% (Table 3). Therefore, the AgNPs/agar/PAN hybrids nanofibers are excellent SERS substrates for detecting MG in water samples.

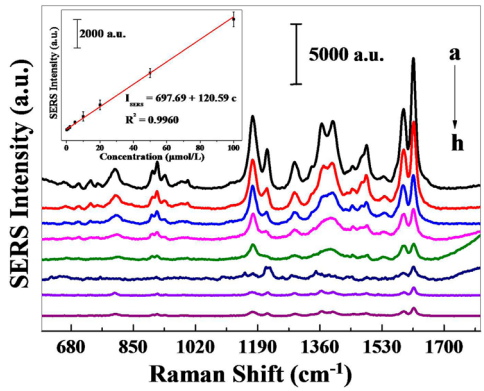

Figure 7. Results of calibration curves: SERS spectra of MG recorded on the AgNPs/agar/PAN nanocomposite fibers at various standard solution concentrations: (a) 100, (b) 50, (c) 20, (d) 10, (e) 5, (f) 2, (g) 1, and (h) 0.1 μmol/L. The top left insert is the calibration curves: the relationships of SERS peak intensities (band 1618 cm^{-1}) and the above concentrations of MG. Laser wavelength, 532 nm; power, 28 mW; lens, 50× objective; acquisition time, 5 s.

Table 3. Results for the Determination of MG in Three Different Water Samples by the Proposed Method[a]

no.	sample	added (μmol/L)	total found (μmol/L)	recovery (%)	RSD (%, *n*=3)
sample 1	fishery water 1	20	19.7 ± 0.9	98.3	4.6
	fishery water 2	20	20.2 ± 0.9	101.1	4.3
sample 2	lake water	20	19.7 ± 1.3	98.5	6.5
		50	50.4 ± 0.9	100.8	1.9
sample 3	river water	20	20.2 ± 0.8	101.0	4.0
		50	50.1 ± 0.6	100.3	2.3

[a]The impurities of the collected water samples were filtered by 0.45 μm filter film after boiling and then stored at room temperature. The determination of MG was measured by SERS after immersing in 1 mL water samples and spiked water samples, respectively. (mean ± SD, n = 3, n = number of each sample tested.).

CONCLUSIONS

In conclusion, we have successfully fabricated the AgNPs/agar/PAN composite nanofibrous mats by a convenient, facile and cost-effective electrospinning technique. Wherein, H-bonds effect between agar and PAN had played a vital role on forming composite mats. In addition, owing to the chelation between the hydroxyl sites of agar and Ag^+, the contents and regular distributions of silver ions (Ag^+) in the polymers get improved and thus the *in situ* photoreductive reaction can effectively occur, resulting in high yield of stable AgNPs with highly uniform and dispersion in the agar/PAN nanofibers. The novel

DOI: 10.1021/am507010q
ACS Appl. Mater. Interfaces 2015, 7, 1586−1594

material, $AgNO_3$/agar/PAN nanofiber mats illuminated by 365 nm UV-lamp, has been successfully demonstrated as a useful hybrid and reproducible SERS substrate for applying to the quantitative determination of MG. Ultimately, the multicomponent functionalized nanofibers based on water-soluble substances integrated with hydrophobic substances may pave the way in developing a hybrid novel membrane for other sensors, catalytic fields, and significantly wider use on a broad range of application in many fields.

■ ASSOCIATED CONTENT

Supporting Information

Additional data and information as noted in the text. This material is available free of charge via the Internet at http://pubs.acs.org.

■ AUTHOR INFORMATION

Corresponding Author

*E-mail: chengzhi@swu.edu.cn. Tel: (+86) 23 68254659. Fax: (+86) 23 68367257.

Notes

The authors declare no competing financial interest.

■ ACKNOWLEDGMENTS

This work was financially supported by the Natural Science Foundation of China (21035005), the found of Chongqing Fundamental and the Cultivation Plan of Chongqing Science & Technology Commission for 100 Outstanding Science and Technology Leading Talents.

■ REFERENCES

(1) Kneipp, J.; Kneipp, H.; Kneipp, K. SERS — a Single-molecule and Nanoscale Tool for Bioanalytics. *Chem. Soc. Rev.* **2008**, *37*, 1052–1060.

(2) Lee, C. H.; Tian, L.; Singamaneni, S. Paper-Based SERS Swab for Rapid Trace Detection on Real-World Surfaces. *ACS Appl. Mater. Interfaces* **2010**, *2*, 3429–3435.

(3) Wei, H.; Xu, H. Hot Spots in Different Metal Nanostructures for Plasmon-enhanced Raman Spectroscopy. *Nanoscale* **2013**, *5*, 10794–10805.

(4) Cui, Q.; Yashchenok, A.; Zhang, L.; Li, L.; Masic, A.; Wienskol, G.; Möhwald, H.; Bargheer, M. Fabrication of Bifunctional Gold/Gelatin Hybrid Nanocomposites and Their Application. *ACS Appl. Mater. Interfaces* **2014**, *6*, 1999–2002.

(5) Tian, Z. Q.; Ren, B.; Li, J. F.; Yang, Z. L. Expanding Generality of Surface-enhanced Raman Spectroscopy with Borrowing SERS Activity Strategy. *Chem. Commun.* **2007**, *44*, 3514–3534.

(6) Wang, Y.; Zhang, J.; Jia, H.; Zeng, J.; Yang, B.; Zhao, B.; Xu, W. Mercaptopyridine Surfaces-Functionalized CdTe Quantum Dots with Enhanced Raman Scattering Properties. *J. Phys. Chem. C* **2008**, *112*, 996–1000.

(7) Carrillo-Carrión, C.; Armenta, S.; Simonet, B. M.; Valcárcel, M.; Lendl, B. Determination of Pyrimidine and Purine Bases by Reversed-Phase Capillary Liquid Chromatography with At-Line Surface-Enhanced Raman Spectroscopic Detection Employing a Novel SERS Sbustrate Based on ZnS/CdSe Silver-Quantum Dots. *Anal. Chem.* **2011**, *83*, 9391–9398.

(8) Tan, Y.; Gu, J.; Xu, W.; Chen, Z.; Liu, D.; Liu, Q.; Zhang, D. Reduction of CuO Butterfly Wing Scales Generates Cu SERS Substrates for DNA Base Detection. *ACS Appl. Mater. Interfaces* **2013**, *5*, 9878–9882.

(9) Ling, J.; Li, Y. F.; Huang, C. Z. Visual Sandwich Immunoassay System on the Basis of Plasmon Resonance Scattering Signals of Silver Nanoparticles. *Anal. Chem.* **2009**, *81*, 1707–1714.

(10) Yang, S.; Cai, W.; Kong, L.; Lei, Y. Surface Nanometer-Scale Patterning in Realizing Large-Scale Ordered Arrays of Metallic Nanoshells with Well-Defined Structures and Controllable Properties. *Adv. Funct. Mater.* **2010**, *20*, 2527–2533.

(11) Zhang, M.; Zhao, A.; Li, D.; Sun, H.; Wang, D.; Guo, H.; Gao, Q.; Tao, W. Generalized Green Synthesis of Diverse LnF_3-Ag Hybrid Architectures and Their Shape-dependent SERS performance. *RSC Adv.* **2014**, *4*, 9205–9212.

(12) Liang, H.; Li, Z.; Wang, W.; Wu, Y.; Xu, H. Highly Surface-roughened "Flower-like" Silver Nanoparticles for Extremely Sensitive Substrates of Surface-enhanced Raman Scattering. *Adv. Mater.* **2009**, *21*, 4614–4618.

(13) Zou, X.; Silva, R.; Huang, X.; Al-Sharab, J. F.; Asefa, T. A Self-cleaning Porous TiO_2—Ag Core-shell Nanocomposite Material for Surface-enhanced Raman Scattering. *Chem. Commun.* **2013**, *49*, 382–384.

(14) He, D.; Hu, B.; Yao, Q. F.; Wang, Y.; Yu, S. H. Large-Scale Synthesis of Flexible Free-Standing SERS Substrates with High Sensitivity: Electropun PVA Nanofibers Embedded with Controlled Alignment of Silver Nanoparticles. *ACS Nano* **2009**, *3*, 3993–4002.

(15) Zhang, C. L.; Yu, S. H. Nanoparticles Meet Electrospinning: Recent Advances and Future Prospects. *Chem. Soc. Rev.* **2014**, *43*, 4423–4448.

(16) Lin, J.; Wang, X.; Ding, B.; Yu, J.; Sun, G.; Wang, M. Biomimicry *via* Electrospinning. *Crit. Rev. Solid State* **2012**, *37*, 94–114.

(17) Sun, B.; Long, Y. Z.; Chen, Z. J.; Liu, S. L.; Zhang, H. D.; Zhang, J. C.; Han, W. P. Recent Advances in Flexible and Stretchable Electonic Devices *via* Electrospinning. *J. Mater. Chem. C* **2014**, *2*, 1209–1219.

(18) Wei, J.; Yang, S.; Wang, L.; Wang, C.; Chen, L.; Chen, S. Electrospun Fluorescein-embedded Nanofivers towards Fingerprint Recognition and Luminescent Patterns. *RSC Adv.* **2013**, *3*, 19403–19408.

(19) Wang, H.; Wang, D.; Peng, Z.; Tang, W.; Li, N.; Liu, F. Assembly of DNA-functionalized Gold Nanoparticles on Electrospun Nanofibers as a Fluorescent Sensor for Nucleic Acids. *Chem. Commun.* **2013**, *49*, 5568–5570.

(20) Wu, D.; Han, D.; Steckl, A. J. Immunoassay on Free-Standing Electrospun Membranes. *ACS Appl. Mater. Interfaces* **2010**, *2*, 252–258.

(21) Thavasi, V.; Singh, G.; Ramakrishna, S. Electrospun Nanofibers in Energy and Environmental Application. *Energy Environ. Sci.* **2008**, *1*, 205–221.

(22) Zhang, L.; Gong, X.; Bao, Y.; Zhao, Y.; Xi, M.; Jiang, C.; Fong, H. Electrospun Nanofibrous Membranes Surface-Decorated with Silver Nanoparticles as Flexible and Active/Sensitive for Surface-enhanced Raman Scattering. *Langmuir* **2012**, *28*, 14433–14440.

(23) Zhao, Y.; Sun, L.; Xi, M.; Feng, Q.; Jiang, C.; Fong, H. Electrospun TiO2 Nanofelt Surface-Decorated with Ag Nanoparticles as Sensitive and UV-Cleanable Substrate for Surface Enhanced Raman Scattering. *ACS Appl. Mater. Interfaces* **2014**, *6*, 5759–5767.

(24) Fathima, S. J. H.; Paul, J.; Valiyaveettil, S. Surface-Structured Gold-Nanotube Mats: Fabrication, Charaterization, and Application in Surface-Enhanced Raman Scattering. *Small* **2010**, *6*, 2443–2447.

(25) He, H.; Cai, W.; Lin, Y.; Dai, Z. Silver Porous Nanotube Built Three-Dimensional Films with Structural Tunability Based on the Nanofiber Template-Plasma Etching Strategy. *Langmuir* **2011**, *27*, 1551–1555.

(26) Bao, Y.; Lai, C.; Zhu, Z.; Fong, H.; Jiang, C. SERS-Active Silver Nanoparticles on Electrospun Nanofibers Facilitated via Oxygen Plas ma Etching. *RSC Adv.* **2013**, *3*, 8998–9004.

(27) Yang, H.; Gao, P. F.; Wu, W. B.; Yang, X. X.; Zeng, Q. L.; Li, C.; Huang, C. Z. Antibacterials Loaded Electrospun Composite Nanofibers: Release Profile and Sustained Antibacterial efficiency. *Polym. Chem.* **2014**, *5*, 1965–1975.

(28) Yang, H.; Huang, C. Z. Polymethacrylic Acid – Facilitated Nanofiber Matrix Loading Ag Nanoparticles for SERS Measurements. *RSC Adv.* **2014**, *4*, 38783–38790.

DOI: 10.1021/am507010q
ACS Appl. Mater. Interfaces 2015, 7, 1586–1594

(29) Guerrero, P.; Etxabide, A.; Leceta, I.; Peñalba, M.; Caba, K. Extraction of Agar from Gelidium *Sesquipedale (Rodhopyta)* and Surface Characterization of Agar Based Films. *Carbohydr. Polym.* **2014**, *99*, 491−498.
(30) Zhu, H.; Du, M. L.; Zhang, M.; Wang, P.; Bao, S. Y.; Wang, L. N.; Fu, Y. Q.; Yao, J. M. Facile Fabrication of AgNPs/(PVA/PEI) Nanofibers: High Electrochemical Efficiency and Durability for Biosensors. *Biosens. Bioelectron.* **2013**, *49*, 210−215.
(31) Witthaut, M.; Cremer, R.; Reichert, K.; Neuschütz, D. Preparation of Cr_2O_3-Al_2O_3 Solid Solutions by Reactive Magnetron Sputtering. *Mikrochim. Acta* **2000**, *133*, 191−196.
(32) Pereira, L.; Sousa, A.; Coelho, H.; Amado, A. M.; Ribeiro-Claro, P. J. A. Use of FTIR, FT-Raman and ^{13}C-NMP Spectroscopy for Identification of Some Seaweed Phycocolloids. *Biomol. Eng.* **2003**, *20*, 223−228.
(33) Chen, H. M.; Yu, D. G. An Elevated Temperature Electrospinning Process for Preparing Acyclovir-loaded PAN Ultrafine Fibers. *J. Mater. Process. Technol.* **2010**, *210*, 1551−1555.
(34) Kubo, S.; Kadla, J. F. Hydrogen Bonding in Lignin: A Fourier Transform Infrared Model Compound Study. *Biomacromolecules* **2005**, *6*, 2815−2821.
(35) Zou, M. L.; Du, M. L.; Zhu, H.; Xu, C. S.; Li, N.; Fu, Y. Q. Synthesis of Silver Nanoparticles in Electrospun Polyacrylonitrile Nanofibers Using Tea Polyphenols as the Reductant. *Polym. Eng. Sci.* **2013**, *53*, 1099−1108.
(36) Rujitanaroj, P.; Pimpha, N.; Supaphol, P. Preparation, Characterization, and Antibacterial Properties of Electrospun Polyacrylonitriles Fibrous Membranes Containing Silver Nanoparticles. *J. Appl. Polym. Sci.* **2010**, *116*, 1967−1976.
(37) Guo, T. L.; Li, G. J.; Ping, X.; Sakka, Y. Controlled Photocatalytic Growth of Ag Nanocrystals on Brookite and Rutile and Their SERS Performance. *ACS Appl. Mater. Interfaces* **2014**, *6*, 236−243.
(38) Braun, G.; Lee, S. J.; Dante, M.; Nguyen, T. Q.; Moskovits, M.; Reich, N. Surface-Enhanced Raman Spectroscopy for DNA Detection by Nanoparticle Assembly onto Smooth Metal Films. *J. Am. Chem. Soc.* **2007**, *129*, 6378−6379.
(39) Pal, J.; Ganguly, M.; Dutta, S.; Mondal, C.; Negishi, Y.; Pal, T. Hierarchical Au-CuO Nanocomposite from Redox Transformation Reaction for Surface Enhanced Raman Scattering and Clock Reaction. *CrystEngComm* **2014**, *16*, 883−893.
(40) Huang, Y. F.; Wu, D. Y.; Zhu, H. P.; Zhao, L. B.; Liu, G. K.; Ren, B.; Tian, Z. Q. Surface-enhanced Raman Spectroscopic Study of *p*-aminothiophenol. *Phys. Chem. Chem. Phys.* **2012**, *14*, 8485−8497.
(41) Hu, X.; Wang, T.; Wang, L.; Dong, S. Surface-Enhanced Raman Scattering of 4-Aminothiophenol Self-Assembled Monolayers in Sandwich Structure with Nanoparticle Shape Dependence: Off-Surface Plasmon Resonance Condition. *J. Phys. Chem. C* **2007**, *111*, 6962−6969.
(42) Fu, W. L.; Zhen, S. J.; Huang, C. Z. One-pot Green Synthesis of Graphene Oxide/Gold Nanocomposites as SERS Substrates for Malachite Green Detection. *Analyst* **2013**, *138*, 3075−3081.
(43) Zhang, B.; Wang, H.; Lu, L.; Ai, K.; Zhang, G.; Cheng, X. Large-Area Silver-Coated Silicon Nanowire Arrays for Molecular Sensing Using Surface-Enhanced Raman Spectroscopy. *Adv. Funct. Mater.* **2008**, *18*, 2348−2355.
(44) Ruan, C.; Eres, G.; Wang, W.; Zhang, Z.; Gu, B. Controlled Fabrication of Nanopillar Arrays as Active Substrates for Surface-Enhanced Raman Spectroscopy. *Langmuir* **2007**, *23*, 5757−5760.
(45) Tan, E. Z.; Yin, P. G.; You, T.; Wang, H.; Guo, L. Three Dimensional Design of Large-Scale TiO_2 Nanorods Scaffold Decorated by Silver Nanoparticles as SERS Sensor for Ultrasensitive Malachite Green Detection. *ACS Appl. Mater. Interfaces* **2012**, *4*, 3432−3437.

DOI: 10.1021/am507010q
ACS Appl. Mater. Interfaces 2015, 7, 1586−1594